Kinetics and Mechanism of NH_3 Formation by the Hydrogenation of Atomic Nitrogen on Rh(111)

R. M. van Hardeveld, R. A. van Santen, and J. W. Niemantsverdriet*

Schuit Institute of Catalysis, Eindhoven University of Technology, P.O. Box 513, 5600 MB Eindhoven, The Netherlands

Received: October 1, 1996; In Final Form: December 3, 1996[⊗]

The reaction between atomic nitrogen and H_2 has been studied in order to elucidate the mechanism of NH_3 formation on Rh(111). Atomic nitrogen layers of 0.10 monolayer (ML) coverage were obtained by adsorbing NO at 120 K and selectively removing the atomic oxygen from dissociated NO by reaction with H_2 at 375 K. The rate of NH_3 formation is first order in the atomic nitrogen coverage and linearly proportional to the H_2 pressure below 5×10^{-7} mbar. Static secondary ion mass spectrometry (SSIMS) indicates that N and NH_2 are the predominant reaction intermediates, while small amounts of NH_3 are also detected. The NH_2 surface coverage increases with increasing H_2 pressure. The presence of NH_2 is also indicated by the appearance of a reaction-limited H_2 desorption state in temperature-programmed desorption (TPD) spectra. The hydrogenation of NH_2 to NH_3 is expected to be the rate-determining step in the NH_3 formation. From the temperature dependence of the NH_3 formation rate an effective activation energy of 40 kJ/mol was determined, which could be translated into an activation energy of 76 kJ/mol for the hydrogenation from NH_2 to NH_3.

Introduction

The reduction of NO_x on rhodium is one of the key reactions that occurs in the automotive exhaust gas convertor. Although the greater part of the NO is reduced by reaction with CO, a substantial part is reduced by hydrogen, which is present in exhaust gas and is moreover formed on the surface of the metal particles by the decomposition of hydrocarbons.[1,2] NO reduction by H_2 may yield three different N-containing products, viz. N_2, N_2O, and NH_3, of which the last two are undesirable from an environmental point of view.

Kinetic studies of the NO + H_2 reaction have been performed on Pt foil,[3] Rh foil,[4] Pt/Rh single crystals,[5,6] Rh/SiO_2,[7] and Rh/Al_2O_3.[8] These studies have shown that the reactivity of atomic nitrogen, which is formed by the dissociation of NO, plays a key role in the selectivity issue of the NO + H_2 reaction. Whereas reactions such as the NO dissociation[9−11] and recombination of atomic nitrogen to N_2[12,13] have been studied extensively, the microscopic mechanisms of N_2O and NH_3 formation are still unknown. NH_3 formation is commonly described by the stepwise hydrogenation of atomic nitrogen.[14] Indeed, many reports on NH and NH_x species exist. On Rh(100)[15] and Pt/Rh(100)[6,16] evidence was found by electron energy loss spectroscopy (EELS) for an NH intermediate that was reversibly formed when a $c(2 \times 2)$-N adlayer was exposed to H_2. Zemlyanov et al.[17] observed an NH intermediate during the NO + H_2 reaction on Pt(100) by EELS. Prasad and Gland[18] explained the formation of diimide N_2H_2 during the decomposition of NH_3 and N_2H_4 on Rh foil by the coupling of NH species on the surface. NH_x intermediates were also observed in NH_3 and N_2H_4 decomposition studies on Ni,[19,20] Pt,[21] Rh,[22,23] and Ru.[24]

Recently, the NO + H_2 reaction regained interest in the context of chemical waves and oscillations that develop under specific reaction conditions on Rh single-crystal planes.[25−30] Cholach et al.[30] concluded that the moving wave front, as observed in field emission microscopy (FEM), represents the hydrogenation of the atomic nitrogen layer followed by the decomposition and/or dissociation of NH_x species into N_2.

The purpose of this paper is to reveal the mechanism of NH_3 formation on Rh(111). Since the details of the NH_3 formation in the NO + H_2 reaction are concealed by simultaneously running reactions such as NO dissociation, N_2, and H_2O formation, we have chosen to study the NH_3 formation starting from a well-defined atomic nitrogen layer.

Since N_2 does not dissociate on Rh(111),[31] an alternative route has to be employed to deposit atomic nitrogen on the surface. The literature reports a number of methods for the preparation of atomic nitrogen layers. Belton et al.[13] prepared N_{ads} layers by dissociation of NO with an electron beam and a subsequent removal of O_{ads} by reaction with CO. Bugyi et al.[12] used a discharge tube to atomize nitrogen before adsorption. Another alternative to preparing N_{ads} layers is exposure of the surface to NH_3 at temperatures above ∼400 K.[32−34] All the above-mentioned preparation methods have the disadvantage that it is difficult to deposit a well-defined amount of atomic nitrogen. Since we want to derive the rate of ammonia formation indirectly from the decrease of the atomic nitrogen coverage, it is essential to know the initial N_{ads} coverage accurately. For this reason, we have prepared atomic nitrogen layers by adsorbing NO at low temperature and removing the O atoms selectively by reaction with H_2 at temperatures where N atoms are not yet hydrogenated or desorbed as N_2. Finally, secondary ion mass spectrometry (SIMS), applied under reaction conditions, reveals that $NH_{2,ads}$ is the dominant NH_x species on the surface during the N hydrogenation.

Experimental Section

Temperature-programmed desorption (TPD) and SIMS experiments were done in a stainless steel ultrahigh vacuum (UHV) system pumped with a 360 L/s turbomolecular pump and a water-cooled titanium sublimation pump. The base pressure was typically around 5×10^{-11} mbar, and mass spectra of the residual gas indicated the presence of mainly H_2, CO, and CO_2. The system is equipped with a Leybold SSM 200 quadrupole

* Corresponding author. Telephone:+31.402473067. Fax: +31.40.2455054. E-mail: tgtahn@chem.tue.nl.

⊗ Abstract published in *Advance ACS Abstracts,* January 1, 1997.

S1089-5647(96)03022-2 CCC: $14.00

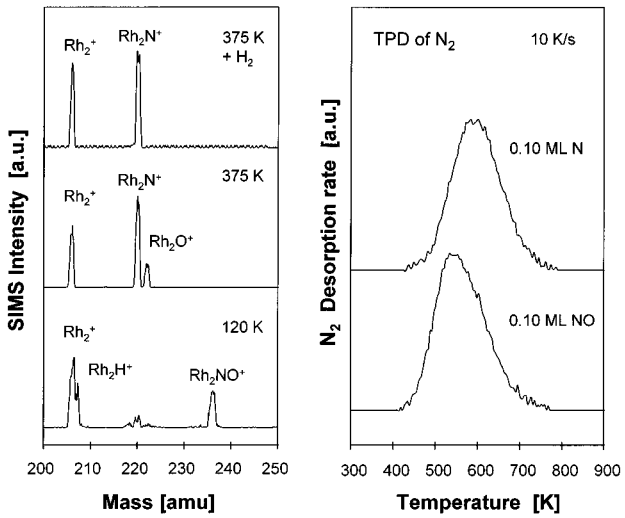

Figure 1. Left panel shows SIMS spectra of the Rh(111) surface after the different reaction steps to produce N_{ads}: molecular NO adsorption at 120 K, thermal NO dissociation at 375 K, and reaction with H_2 to remove atomic oxygen. The right panel shows a comparison between the N_2 TPD spectra obtained from a surface covered with 0.10 ML atomic nitrogen and 0.10 ML NO. The absence of atomic oxygen results in a shift of the N_2 desorption maximum to higher temperature.

mass spectrometer for TPD and SIMS and a Leybold EA 10 hemispherical energy analyzer for Auger electron spectroscopy (AES) and $\Delta\varphi$ measurements. Both analyzers are interfaced with a PC for data storage.

SIMS measurements were carried out in the static (low-damage) mode. Typically, we used a defocused 5 keV primary Ar^+ beam with a current density of $1-10$ nA/cm^2. To average eventual anisotropies in the secondary ion emission process, we applied a target bias of $+45$ V and an extractor voltage of -300 V on the entrance lens of the quadrupole system.

The UHV system contained a rhodium crystal that was cut in the [111] orientation within 0.5° and polished according to standard procedures. The temperature was measured by a chromel−alumel thermocouple spot-welded on the back of the crystal. The standard cleaning procedure consisted of an argon sputter treatment (900 K, 1.5 keV, 5 μA/cm^2) followed by annealing in 2×10^{-8} mbar O_2 (900−1100 K) and a final annealing treatment in vacuum at 1420 K. The gases, NO (Messer Griesheim, 99.5%) and H_2 (Messer Griesheim, 99.995%), were used without further treatment. Exposures are reported in langmuirs (1 langmuir $= 1.33 \times 10^{-6}$ mbar•s), and coverages are expressed with respect to the number of Rh surface atoms (1 monolayer (ML) $=1.6 \times 10^{15}$ cm^{-2}).

Atomic nitrogen layers with a coverage of 0.10 ML were obtained by adsorbing 0.25 langmuir NO at 120 K and selectively removing the atomic oxygen at 375 K by reaction with 2×10^{-8} mbar hydrogen during 160 s. The atomic nitrogen layers were exposed to H_2 at various pressures and temperatures. The amount of nitrogen remaining after the hydrogenation experiment was determined by TPD. Although the surface also contained NH_x intermediates, N_2 was the only nitrogen-containing desorption product observed. We mention here that the experiments were only possible with an excellent background pressure ($p < 5 \times 10^{-11}$ mbar), where CO adsorption during the reaction procedure can be prevented.

Results

Preparation of Atomic Nitrogen Layers on Rh(111). For all the experiments we started from an atomic nitrogen layer with a coverage of 0.10 ML (±3%). Figure 1 illustrates the procedure for preparing atomic nitrogen with SIMS spectra of the Rh(111) surface after NO adsorption at 120 K, heating to 375 K to dissociate the NO, and after reaction with hydrogen at 375 K to remove the oxygen.

The presence of molecularly adsorbed NO at 120 K is indicated in the SIMS spectrum by the appearance of the Rh_2NO^+ cluster ion at $m/e = 236$. Heating to 375 K results in complete dissociation of the adsorbed NO molecules. This is evidenced by the appearance of the Rh_2N^+ and Rh_2O^+ cluster ions (at $m/e = 220$ and $m/e = 222$), which are representative for atomic N and O, respectively, and by the disappearance of the Rh_2NO^+ cluster ion. The removal of atomic oxygen by reaction with hydrogen is clearly illustrated by the disappearance of the Rh_2O^+ peak. Although removing the oxygen results in a large decrease of the SIMS intensities, the presence of atomic nitrogen remains clearly visible by the Rh_2N^+ peak at $m/e = 220$. Temperature-programmed desorption confirms that the hydrogen treatment to remove the oxygen does not result in a decrease of the atomic nitrogen coverage, since the N_2 TPD peak areas before and after the H_2 reaction are equal. The removal of the atomic oxygen is also illustrated by the N_2 desorption behavior. As Figure 1 shows, removal of atomic oxygen results in a shift of the N_2 desorption spectrum to higher temperature, attributed to the disappearance of repulsive interactions between oxygen and nitrogen atoms on the surface.

Hydrogenation of Atomic Nitrogen at Constant Temperature and H_2 Pressure. In this section we show how the coverage of an atomic nitrogen layer decreases when it is exposed to a constant H_2 pressure at a fixed temperature. The decrease of the atomic nitrogen coverage was determined by comparing the N_2 TPD area after a hydrogenation experiment with the N_2 TPD area of the initial atomic nitrogen layer.

As we will show in the discussion section, hydrogen adsorption is readily at equilibrium under our reaction conditions. We have restricted the upper temperature limit to 400 K in order to prevent N_2 formation and desorption. We found that up to 400 K the atomic nitrogen coverage remained unchanged when the crystal was kept isothermally in vacuum for several minutes. Under these conditions the rate of ammonia formation equals the decrease of the atomic nitrogen coverage and can be written as

$$r_{NH_3} = -d\theta_N/dt = k_{eff}\theta_N{}^n\theta_H{}^m = k'_{eff}\theta_N{}^n \qquad (1)$$

The decrease of the nitrogen coverage with time is determined by the *n*th-order dependence of the ammonia formation rate on the nitrogen coverage. Figure 2 shows the decrease of the nitrogen coverage with time at $T = 375$ K and $p_{H2} = 2 \times 10^{-7}$ mbar and at $T = 400$ K and $p_{H2} = 5 \times 10^{-7}$ mbar. Although the nitrogen coverage continues to decrease below 0.04 ML, the data are not shown in Figure 2, since the relative error in the remaining N_{ads} coverage determination by TPD becomes too large.

The decreasing slope of the θ_N coverage versus time curve indicates a positive order n of the ammonia formation rate in the nitrogen coverage. If the order n is assumed to be unity, integration of eq 1 yields

$$\ln[\theta_N(t)/\theta_N(0)] = -k'_{eff}t \qquad (2)$$

where $\theta_N(t)$ and $\theta_N(0)$ are the nitrogen coverages after and before reaction, respectively. The inset of Figure 3 confirms that a linear relation is obtained if the logarithm of the coverage ratio is plotted versus time. This indicates that the ammonia formation rate is proportional to the nitrogen coverage.

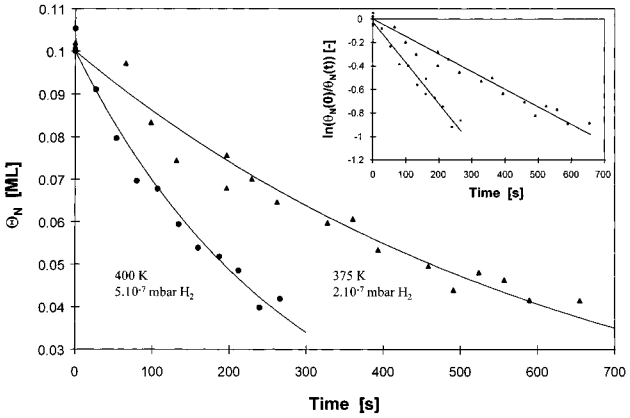

Figure 2. Decrease of the atomic nitrogen coverage with time due to reaction with H_2 at constant temperature and pressure. The inset shows that a linear relation is obtained when the ratio of the initial to remaining atomic nitrogen coverage is plotted versus the time, indicating that the hydrogenation rate is first order in the atomic nitrogen coverage.

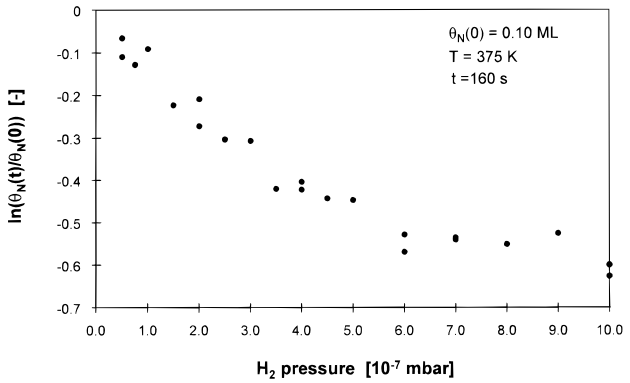

Figure 3. Influence of the H_2 pressure on the hydrogenation rate, indicated by plotting the $\ln(\theta_N(t)/\theta_N(0))$ after 160 s of reaction versus the H_2 pressure. Initially, the hydrogenation rate is linearly proportional to the H_2 pressure, but the dependence levels off above $\sim 5 \times 10^{-7}$ mbar H_2.

Dependence of the NH_3 Formation Rate on the H_2 Pressure. The H_2 pressure dependence of the NH_3 formation rate can give information on the rate-determining step in the subsequent hydrogenation of atomic nitrogen to NH_3.

Under the applied reaction conditions, the hydrogen coverage is expected to be small ($\theta_H \ll 1$), and therefore, it is proportional to the square root of the H_2 pressure. In this case the following general dependence is expected:

$$\ln[\theta_N(t)/\theta_N(0)] = -k_{eff}\theta_H{}^m t = -k''_{eff} p_{H2}{}^{m/2} t \qquad (3)$$

The pressure dependence of the hydrogenation rate was investigated by keeping the reaction time constant at 160 s and varying the H_2 pressure in the range between 2×10^{-8} and 1×10^{-6} mbar. Figure 3 shows a plot of the logarithm of the ratio of the remaining and initial N_{ads} coverage versus the hydrogen pressure at 375 K. The curve shows that for pressures below 5×10^{-7} mbar, the dependence is close to linear whereas the dependence levels off in the pressure range from 5×10^{-7} to 1×10^{-6} mbar. A similar experiment at 400 K showed a similar H_2 pressure dependence.

Based on these results only, assignment of the rate-determining step is not possible. However, we definitely conclude that the first hydrogenation step is not rate limiting. In that case, the H_2 pressure dependence would be at most a square root dependence. Figure 3, however, shows a linear dependence for H_2 pressures below 5×10^{-7} mbar.

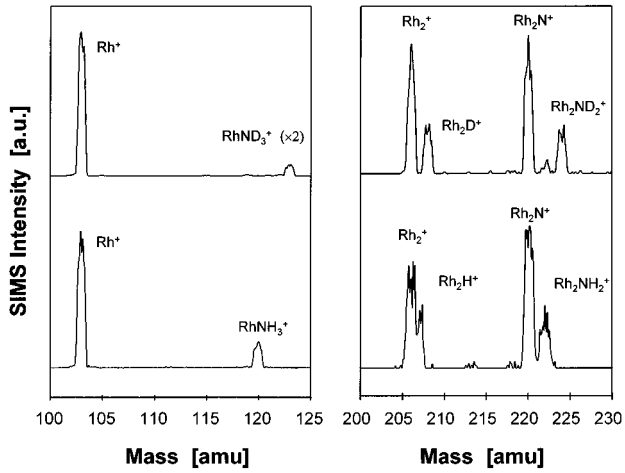

Figure 4. SIMS spectra of the Rh(111) surface during a hydrogenation experiment showing the presence of H (Rh_2H^+ 207 amu), N (Rh_2N^+ 220 amu), NH_2 ($Rh_2NH_2^+$ 222 amu), and NH_3 ($RhNH_3^+$ 120 amu) as reaction intermediates. Peak assignments were verified by using D_2 instead of H_2. The spectrum was taken after 20 s of reaction, the H_2 pressure was 5×10^{-7} mbar, and $T = 375$ K.

Identification of NH_x Reaction Intermediates by SIMS. For elucidating the hydrogenation mechanism of atomic nitrogen to NH_3, the identification of surface intermediates is of great significance. In previous studies, SIMS has successfully been applied to identify NH_x-like intermediates on the surface.[35,36] This section presents the SIMS results of the Rh(111) surface during N hydrogenation. The collection time for a SIMS spectrum was 15 s, which is about 10% of the time scale of a typical hydrogenation experiment. Spectra were taken after 20 s of reaction to be sure that equilibrium was reached between the NH_x intermediates and to compare different reaction conditions with similar nitrogen coverages.

Figure 4 shows two characteristic mass regions of a SIMS spectrum of the Rh(111) surface taken after 20 s of reaction at 5×10^{-7} mbar H_2 and 375 K. The presence of NH_3 on the surface is evidenced by the appearance of the $Rh(NH_3)^+$ cluster ion at $m/e = 120$. In the high-mass range, N_{ads} and $NH_{2,ads}$ are observed as predominant surface species by the appearance of the Rh_2N^+ and $Rh_2(NH_2)^+$ cluster ions at $m/e = 220$ and $m/e = 222$, respectively. From a previous investigation we know that the $Rh_2(NH_2)^+$ cluster ion is *not* a consequence of the presence of NH_3 on the surface.[36] The presence of hydrogen on the surface is evidenced by the appearance of the Rh_2H^+ peak at $m/e = 207$, which is not fully resolved from the Rh_2^+ peak, however. To facilitate the assignment of the SIMS peaks, H_2 was exchanged for D_2, which resulted in the expected mass shifts, as Figure 4 shows. In this case also a small peak at $m/e = 222$ is resolved. Whether this peak stems from the presence of ND on the surface or results from fragmentation of ND_2 is unknown.

Although the presence of N, NH_2, and NH_3 on the surface is clearly established by the spectra in Figure 4, interpretation of the peak intensities in terms of surface coverages is rather complicated. Previous studies have shown that SIMS peak intensity ratios can give quantitative information about coverages of adsorbates.[36−38] However, it should be noted that occasionally nonlinear correlations between intensity ratios and coverage are observed. Therefore, careful calibration is required in order to obtain quantitative information from SIMS measurements. For NH_3 we have been able to do such a calibration by studying the adsorption of NH_3 on Rh(111).[36] In the case of NH_x intermediates, however, calibration is much more difficult, since no methods are at hand to prepare well-defined coverages of

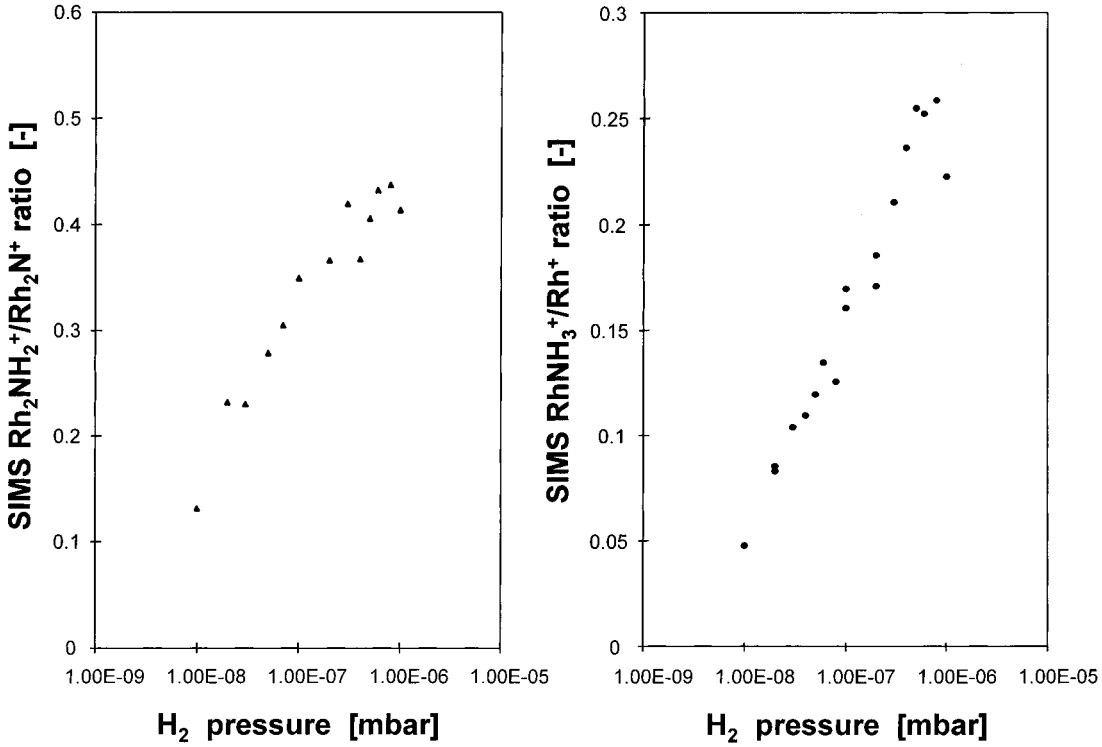

Figure 5. Left panel shows the H_2 pressure dependence of the SIMS $Rh_2NH_2^+/Rh_2N^+$ peak intensity ratio that initially increases with H_2 pressure but reaches a saturation value of ~0.43 above 5×10^{-7} mbar. The right panel shows the dependence of the $RhNH_3^+/Rh^+$ peak intensity ratio, which monotonically increases with the H_2 pressure. In both cases the temperature was 375 K and the SIMS spectra were taken after 20 s of reaction.

NH_x species on the surface. We have therefore assumed that the $Rh_2NH_2^+/Rh_2N^+$ peak ratio reflects at least qualitatively the coverage ratio of NH_2 and N on the surface. The intensity of the Rh_2^+ peak was not used as a reference, since it was not fully resolved from the Rh_2H^+ peak.

Figure 5 shows the H_2 pressure dependence of the $Rh(NH_3)^+/Rh^+$ and $Rh(NH_2)^+/RhN^+$ peak intensity ratios at a constant temperature of 375 K. The SIMS spectra were taken after 20 s of reaction. The $Rh(NH_2)^+/RhN^+$ peak intensity ratio increases in the H_2 pressure regime between 1×10^{-8} and ~5×10^{-7} mbar but becomes constant at higher H_2 pressures. The $Rh(NH_3)^+/Rh^+$ peak intensity ratio increases over the whole pressure regime. Thus, NH_2 is the predominant NH_x species during the hydrogenation of atomic nitrogen while small amounts of NH_3 are present as well. The coverage of both NH_2 and NH_3 increases with increasing H_2 pressure, but for NH_2 the dependence levels off to a constant at a pressure of about 5×10^{-7} mbar.

We have also investigated the influence of the temperature on the presence of the intermediates on the surface. Figure 6 shows the dependence of the $Rh(NH_3)^+/Rh^+$ and $Rh(NH_2)^+/RhN^+$ peak intensity ratios on temperature at a constant H_2 pressure of 1×10^{-6} mbar and also after 20 s of reaction. The $Rh(NH_3)^+/Rh^+$ peak ratio increases somewhat up to temperatures of 365 K, whereafter it decreases rapidly. Except for the measurement at 325 K, the $Rh(NH_2)^+/RhN^+$ peak ratio remains more or less constant over the entire temperature range.

Evidence for NH_x Intermediates from TPD. In the literature, much of the evidence for the existence of NH_x intermediates is based on the appearance of a reaction-limited H_2 desorption state.[23,39,40] To make the comparison to our results, we have frozen the intermediates present under reaction conditions by rapid cooling (4 K/s) under H_2 atmosphere to 275 K, after which the system was evacuated for 2 min and a TPD experiment was performed. Figure 7 shows the H_2 and N_2 TPD spectra obtained by freezing the reaction at 350 K and 5×10^{-7} mbar H_2 after 20 s. The H_2 desorption spectrum clearly shows two desorption states. The low-temperature desorption state with a peak maximum at 330 K represents the common second-order desorption-limited state. The H_2 desorption state with a peak maximum around 415 K corresponds to a reaction-limited state, which is attributed to the decomposition of NH_x intermediates.

The only nitrogen-containing product that was observed during TPD was N_2, whereas no NH_3 and N_2H_2 could be detected. Furthermore, it appeared that all NH_x had decomposed before N_2 desorption started at around 500 K. Figure 7 also shows a SIMS spectrum of the surface *before* TPD was performed, which indicates the presence of N, NH_2, and NH_3 on the surface.

The ratio of the atomic nitrogen coverage to the amount of hydrogen desorbing in the reaction-limited desorption state at 415 K is of interest because it can give additional information about the composition of the NH_x intermediate. Comparison of the N_2 and H_2 TPD peak areas and correcting for differences in ionization probabilities ($S_{H2}/S_{N2} = 0.45$) yields an overall N:H ratio of 1:1.1 for the NH_x intermediates. A different way to determine the N:H ratio is by relating the N_2 and H_2 TPD areas to the NO and H_2 uptake curves. In this way, the atomic nitrogen coverage was estimated to be 0.10 ML and the amount of hydrogen desorbing from the reaction-limited state was 0.11 ML, which results in the same overall N:H ratio of 1:1.1 for the NH_x intermediates.

Note that the H:N ratio of 1.1 reflects the overall composition of the surface after 20 s of hydrogenation at 350 K, excluding the atomic hydrogen, and has no bearing on the composition of the NH_x species themselves.

Dependence of the NH_3 Formation Rate on Temperature. To determine the effective Arrhenius parameters, we investi-

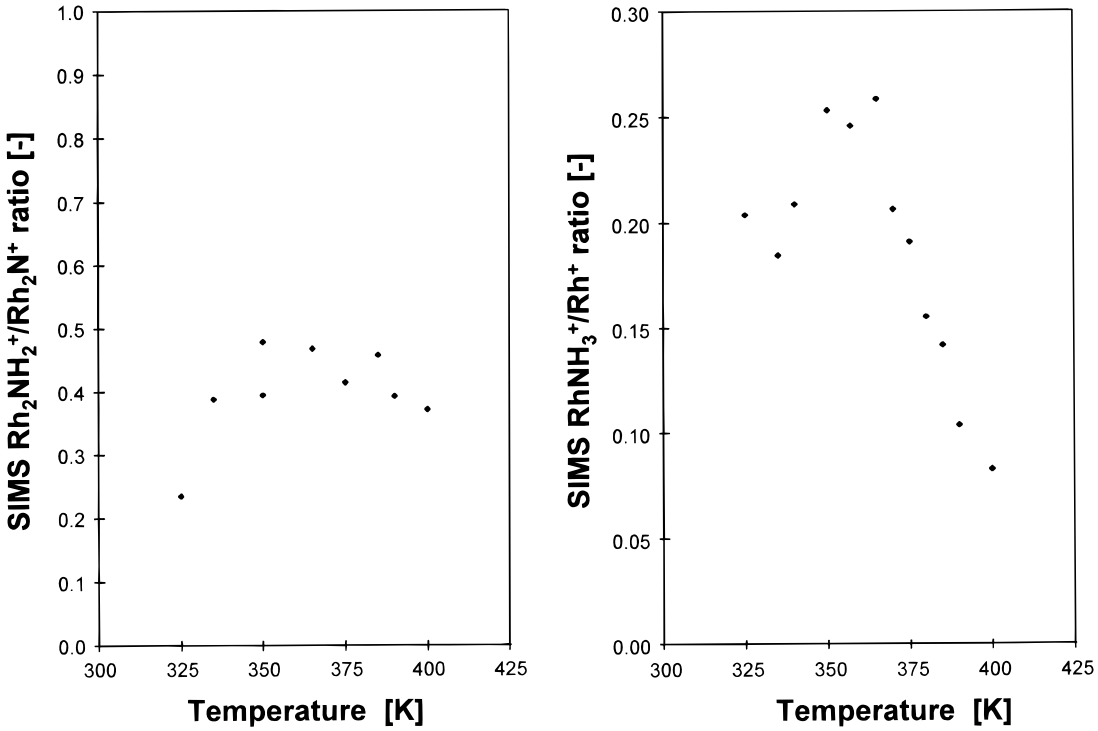

Figure 6. Left panel shows that the SIMS $Rh_2NH_2^+/Rh_2N^+$ peak intensity ratio at a H_2 pressure of 1×10^{-6} mbar is independent of the temperature. The right panel shows that the $RhNH_3^+/Rh^+$ peak intensity ratio first slightly increases with temperature but decreases rapidly above 360 K. SIMS spectra were taken after 20 s of reaction.

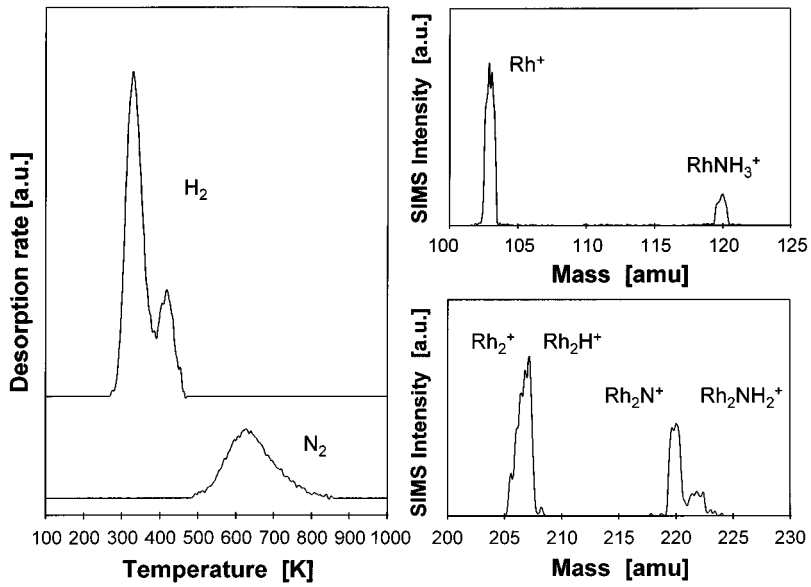

Figure 7. Left panel shows the H_2 and N_2 TPD spectra resulting from an NH_x covered surface that was obtained by cooling to 275 K after 20 s of reaction at 350 K and 5×10^{-7} mbar H_2. The reaction-limited H_2 desorption state at 415 K indicates the presence of NH_x intermediates. Comparison of the H_2 and N_2 peak areas yields an overall N:H surface ratio in the NH_x intermediates of 1:1.1. The right panel shows a SIMS spectrum of the surface before TPD was carried out, indicating the presence of H, N, NH_2, and NH_3.

gated the rate of NH_3 formation in the temperature range 325−400 K. In these experiments the H_2 pressure was kept constant at 1×10^{-6} mbar. Figure 8 shows the logarithm of the hydrogenation rate versus the reciprocal temperature. The slope of the curve corresponds to an effective activation energy of 40 kJ/mol, while the effective pre-exponential equals 10^2 s^{-1}. We use the terms effective activation energy and pre-exponential, since several equilibrium and rate constants may be involved depending on the rate-limiting step. At least the hydrogen adsorption equilibrium has to be incorporated, since the H_2 pressure is kept constant while the temperature changes, which results in varying hydrogen coverages.

Discussion

Mechanism and Kinetic Description of NH_3 Formation on Rh(111). With respect to the kinetic mechanism of the stepwise hydrogenation of atomic nitrogen to NH_3, the following experimental results are pertinent. (1) The rate of ammonia formation is linearly proportional to the hydrogen pressure below 5×10^{-7} mbar H_2. (2) SIMS spectra indicate that N and NH_2 are the predominant surface species under reaction conditions, whereas NH_3 and possibly NH are present only in very small amounts. (3) The reaction-limited H_2 desorption state, emanating from NH_x decomposition, indicates the presence of signifi-

cant amounts of NH_x on the surface under reaction conditions; the average H:N ratio in the NH_x intermediates is 1.1:1.

Concurrently, these results point to the hydrogenation of NH_2 as the rate-determining step. We therefore propose the following sequence of steps with the associated equilibrium constants:

$$H_{2,g} + 2^* \rightleftarrows 2H_{ads} \qquad K_1 = \theta_H{}^2/(\theta_*{}^2 p_{H2}) \qquad (4.1)$$

$$N_{ads} + H_{ads} \rightleftarrows NH_{ads} + * \qquad K_2 = (\theta_{NH}\theta_*)/(\theta_N\theta_H) \qquad (4.2)$$

$$NH_{ads} + H_{ads} \rightleftarrows NH_{2,ads} + * \qquad K_3 = (\theta_{NH2}\theta_*)/(\theta_{NH}\theta_H) \qquad (4.3)$$

$$NH_{2,ads} + H_{ads} \rightarrow NH_{3,ads} + * \qquad r_{NH3} = k_4\theta_{NH2}\theta_H \qquad (4.4)$$

$$NH_{3,ads} \rightarrow NH_{3,g} + * \qquad r_{NH3} = k_5\theta_{NH3} \qquad (4.5)$$

We will justify and discuss this kinetic mechanism in the following. Under our experimental conditions, i.e., $2 \times 10^{-8} < p_{H2} < 1 \times 10^{-6}$ mbar and $325 < T < 400$ K, both the rate of hydrogen adsorption and desorption are fast compared to the NH_3 formation rate. Furthermore, hydrogen adsorption is sufficiently fast to supply hydrogen for the conversion of atomic nitrogen into NH_x species. We therefore conclude that H_2 adsorption rapidly reaches equilibrium (on the order of seconds).

Although initially all the nitrogen on the surface is present as N_{ads}, exposure to hydrogen results in the conversion of part of the atomic nitrogen into NH_x species. It is difficult to determine the exact time scale upon which equilibrium between the NH_x intermediates is reached. However, the rapid buildup of the NH_x intermediates and the absence of an induction period in the time dependent hydrogenation experiments indicate that equilibrium conditions apply for the major part of the time scale of the hydrogenation experiments. In the final step, NH_3 readsorption can be neglected, since the NH_3 production rate is slow compared to the pumping speed of the vacuum system, resulting in a negligible NH_3 background pressure.

Under the assumption that equilibrium conditions apply for both H_2 adsorption and the NH_x intermediates up to NH_2, the following kinetic expression can be derived for the decrease of the nitrogen coverage with time (which is equal to the NH_3 formation rate):

$$\frac{d\theta_{N,tot}(t)}{dt} = -k_4\theta_{NH_2}(t)\theta_H$$

$$\frac{d\theta_{N,tot}(t)}{dt} = -k_4\theta_{N,tot}(t)\frac{K_2K_3(K_1p_{H_2})}{1 + K_2(K_1p_{H_2})^{1/2} + K_2K_3(K_1p_{H_2})}\frac{(K_1p_{H_2})^{1/2}}{1 + (K_1p_{H_2})^{1/2}} \qquad (5)$$

The number of empty sites available for hydrogen adsorption equals

$$\theta_* = 1 - \theta_H - \sum\theta_{NHx}$$

For the derivation of eq 5 we have made the assumption that $\theta_* \approx 1 - \theta_H$. This has the advantage that two independent factors are obtained for the H_2 pressure dependence of the hydrogen adsorption equilibrium and the equilibria of the NH_x intermediates (last and second factor in eq 5, respectively). The choice of the number of empty sites available for hydrogen adsorption is quite arbitrary anyway, so we have assumed it to be unity in accordance with the situation on the empty surface.

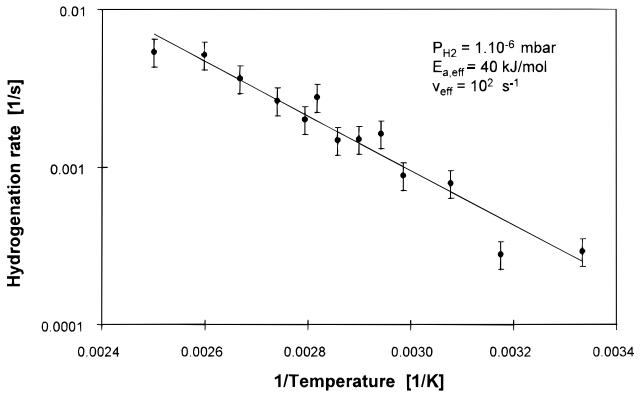

Figure 8. Dependence of the hydrogenation rate, determined as $\ln(\theta_N(0)/\theta_N(t))/t$ after 160 s of reaction at 1×10^{-6} mbar, on the temperature. The effective activation energy was 40 kJ/mol, and the effective pre-exponential was 10^2 s^{-1}.

In fact the number of empty sites increases during the hydrogenation experiment because of the decrease of the nitrogen coverage. However, the decrease of the atomic nitrogen coverage in a typical hydrogenation experiment was on the order of 0.05 ML, and therefore, the increase of the number of empty sites is relatively small. Hence, eq 5 should be valid under the conditions employed in this work.

H_2 Pressure Dependence of the NH_3 Formation Rate. As the second factor in eq 5 indicates, the order in the H_2 pressure of the NH_2 coverage can vary between 0 and 1. As stated previously, the hydrogen coverage is small under our reaction conditions and therefore proportional to $p_{H2}{}^{1/2}$. This can easily be seen from the last factor in eq 5, which represents the hydrogen coverage and reduces to $(K_1p_{H2})^{1/2}$ if $K_1p_{H2} \ll 1$. In consequence of this, the order of the NH_3 formation rate in the H_2 pressure can vary between 1/2 and 3/2 as extremes.

Figure 5 shows that the NH_2 coverage increases with increasing H_2 pressures below $\sim 5 \times 10^{-7}$ mbar, whereas the NH_2 coverage becomes constant at higher H_2 pressures. From a kinetic point of view, the observed H_2 dependence of the NH_2 coverage and the NH_3 formation rate is consistent. At pressures below 5×10^{-7} mbar both the NH_2 and the hydrogen coverage depend on the H_2 pressure, resulting in an overall first-order dependence of the NH_3 formation rate on the H_2 pressure. Above 5×10^{-7} mbar H_2, the NH_2 coverage becomes constant and the H_2 pressure dependence of the NH_3 formation rate is determined solely by the pressure dependence of the hydrogen coverage ($\sim p_{H2}{}^{1/2}$).

Presence of NH_x Intermediates on the Surface under Reaction Conditions. The SIMS results of the surface under reaction conditions indicate that N and NH_2 are the predominant nitrogen surface species. Drechsler et al.,[35] using SIMS, have demonstrated that NH is the main surface species during the NH_3 decomposition on Fe. We may therefore conclude that the absence of NH in our SIMS spectra is not caused by a poor sensitivity but is due to a low surface coverage of NH. NH_3 is also detected but only in very small amounts. A previous study on the adsorption of NH_3 on Rh(111)[36] indicated that an NH_3 coverage as small as 0.01 ML resulted in a SIMS $Rh(NH_3)^+/Rh^+$ peak intensity ratio as large as ~ 7. In the present case the SIMS $Rh(NH_3)^+/Rh^+$ peak intensity ratio does not exceed a value of 0.25 (see Figure 5), which points to a negligibly low coverage. In fact the NH_3 steady-state coverage is determined by the ratio of NH_3 production to the desorption rate:

$$NH_{2,ads} + H_{ads} \xrightarrow{k_4} NH_{3,ads} \xrightarrow{k_5} NH_{3,gas}$$

$$\theta_{NH_3} = \frac{k_4 \theta_{NH_2} \theta_H}{k_5} \quad (6)$$

Under steady-state conditions the rate of NH_3 formation is equal to the rate at which the nitrogen coverage decreases. As Figure 2 shows, a typical value for the decrease of the nitrogen coverage is 0.0002 ML/s. For the NH_3 desorption rate an activation energy of 81.5 kJ/mol was found if a pre-exponential factor of 10^{13} was assumed.[36] By use of these values, an NH_3 steady-state coverage of 4×10^{-6} ML is calculated at 375 K. Since this coverage is very small, we must be conscious about the role that surface defects might play. If NH_3 is for instance adsorbed more strongly to defect sites, the coverage might become significantly higher.

Equation 6 predicts that the NH_3 steady-state coverage increases if the NH_3 formation rate increases. This is in line with the results in Figure 5, which shows that the NH_3 steady-state coverage for a given temperature increases with increasing H_2 pressure.

Since no reference is available, it is difficult to give a precise estimate of the NH_2:N surface coverage ratio on the basis of the SIMS $Rh_2NH_2^+/Rh_2N^+$ peak intensity ratio. Quantification is complicated, since the relative SIMS sensitivities for N and NH_2, and the fragmentation of the $Rh_2NH_2^+$ cluster ion to Rh_2N^+, are unknown. Nevertheless, it is remarkable that the SIMS $Rh_2NH_2^+/Rh_2N^+$ peak intensity ratio becomes independent of the H_2 pressure above 5×10^{-7} mbar at 375 K (see Figure 5, and note the logarithmic pressure scale) and is also independent of the temperature at a constant H_2 pressure of 1×10^{-6} mbar (see Figures 6). In all cases the $Rh_2NH_2^+/Rh_2N^+$ peak intensity ratio saturated at a value of $\sim$0.43. This might indicate that not all nitrogen is accessible to hydrogen. Yamada et al.[15] reported that hydrogen exposure to a $c(2 \times 2)$-N adlayer on Rh(100) only resulted in NH_x formation at the edges of nitrogen islands. From our results we have no direct evidence for island formation, but it could explain why the NH_2 coverage saturates while the $Rh_2NH_2^+/Rh_2N^+$ ratio remains small.

In the literature most of the information concerning the stability of NH_x intermediates stems from decomposition experiments. Bassignana et al.[20] showed that on Ni(110) NH_2 is the predominant intermediate formed during thermal NH_3 decomposition at 350 K. An activation energy of 20 kcal/mol was reported for NH_2 decomposition into N or NH. Also, Rausher et al.[24] reported NH_2 as a stable intermediate on Ru(001) between 280 and 300 K during N_2H_4 decomposition. The NH_2 intermediate was found to decompose into NH at higher temperatures. On Rh(111), Wagner and Schmidt[22] reported a reaction-limited H_2 desorption peak at 430 K when studying the reactions of oxygen with NH_3 and N_2H_4. This reaction-limited H_2 desorption peak seems identical with the one we observed during TPD of the Rh(111) surface containing the NH_x intermediates formed during the hydrogenation of N_{ads} (see Figure 7). However, Wagner and Schmidt attributed the H_2 formation to decomposition of NH rather than to NH_2. This latter assignment has been made in a previous investigation by the same authors Wagner and Schmidt,[41] where they investigated the decomposition of H_2NCHO, D_2NCHO, N_2H_4, and NH_3 on Rh(111). Decomposition of D_2NCHO showed that the reaction-limited H_2 (D_2) peak at 430 K stemmed from decomposition of the amino NH_2 (ND_2) group. Similar to our findings, they determined an overall N:H ratio of 1:1.08 when comparing the N_2 and reaction-limited H_2 (D_2) desorption peak areas. From this result they concluded that decomposing NH_x species was NH. A reaction-limited NH_3 desorption state was also observed in these experiments, which was explained by hydrogenation of NH_2. It should be noted that their results could of course also be explained by assuming that the surface contained N and NH_2 in a 1:1 ratio.

Kinetic Parameters of NH_3 Formation. Figure 7 shows that at a H_2 pressure of 1×10^{-6} mbar the $Rh_2NH_2^+/Rh_2N^+$ peak ratio is almost independent of the temperature and equal to the saturation value. If we assume that the $Rh_2NH_2^+/Rh_2N^+$ peak ratio is a measure of the NH_2 coverage, the latter is also temperature independent. This greatly simplifies the interpretation of the measured activation energy, since the temperature dependence of the NH_2 equilibrium is not incorporated. In this case, the effective rate constant that is measured equals the product of the elementary rate constant for the reaction from NH_2 to NH_3 and the square root of the H_2 adsorption equilibrium constant, $k_{eff} = k_4 K_1^{1/2}$ (see eq 5). Under these assumptions, the activation energy for the reaction of NH_2 to NH_3 equals

$$E_{act,NH_2 \rightarrow NH_3} = E_{act,eff} + {}^1/_2 E_{des,H_2} = 40 + 36 = 76 \text{ [kJ/mol]} \quad (7)$$

H_2 TPD experiments yielded an activation energy and pre-exponential of 72 kJ/mol and 10^{11} s^{-1}, respectively, for desorption in the low-coverage limit, in good agreement with the literature.[42]

The only activation energy reported in the literature on NH_3 formation stems from Hirano et al.[5] They found an effective activation energy of 55 kJ/mol for NH_3 formation by the reaction of $NO + H_2$ on a $Pt_{0.25}-Rh_{0.75}(100)$ single crystal. Comparison with our value is difficult, since it is not clear which reaction constants contribute to the effective activation energy. Shustorovich and Bell[43] have studied the synthesis and decomposition of NH_3 on transition metal surfaces by a bond-order-conservation-Morse-potential analysis and concluded that the first hydrogenation step, i.e., the reaction from N to NH, is rate limiting in NH_3 formation on Pt. Furthermore, they concluded that both NH_2 and NH_3 are more stable surface intermediates than NH and that NH_3 desorption is favored above NH_3 decomposition. Although the calculations are performed for Pt(111), the discrepancies with our findings and those of other authors are striking. First, it contradicts the H_2 pressure dependence we observed for the NH_3 formation rate on Rh(111), and second, it cannot explain the buildup of significant amounts of NH_x intermediates, either during NH_3 decomposition or NH_3 formation.

Conclusions

Atomic nitrogen layers with well-determined coverage can be prepared by adsorbing NO at low temperature followed by thermal dissociation and selective removal of the atomic oxygen by reaction with hydrogen. When the atomic nitrogen layer is exposed to H_2 at constant temperature and pressure, the rate at which the atomic nitrogen coverage decreases appears to be first order in the atomic nitrogen coverage. The rate of NH_3 formation is first order in the H_2 pressure between 1×10^{-8} and 5×10^{-7} mbar, but the order decreases between 5×10^{-7} and 1×10^{-6} mbar. SIMS spectra of the surface under reaction conditions indicate, by the appearance of Rh_2N^+ and $Rh_2NH_2^+$ peaks at $m/e = 220$ and *222*, respectively, that N and NH_2 are the predominant surface intermediates. Small amounts of NH_3 could be monitored on the surface by the appearance of the $RhNH_3^+$ cluster ion in the SIMS spectra. The NH_2 coverage increased with increasing H_2 pressure between 1×10^{-8} and 5×10^{-7} mbar at 375 K. In the pressure range between 5×10^{-7} and 1×10^{-6} mbar the NH_2 coverage became constant. At a pressure of 1×10^{-6} mbar H_2, the NH_2 steady-state

coverage was independent of the temperature. The presence of NH_x species was also evidenced by the appearance of a reaction-limited H_2 desorption state at 415 K attributed to decomposition of NH_2.

From the temperature dependence of the NH_3 formation rate, an effective pre-exponential and activation energy of 10^2 s^{-1} and 40 kJ/mol were calculated. The experimental results can best be explained by assuming that the third hydrogenation step, i.e., the hydrogenation from NH_2 to NH_3, is rate limiting. The activation energy of this step is 76 kJ/mol.

References and Notes

(1) Taylor, K. C. *Catal. Rev. Sci. Eng.* **1993**, *35*, 457.
(2) Kobylinski, T. P.; Taylor, B. W. *J. Catal.* **1974**, *33*, 376.
(3) Papapolymerou, G.; Botis, A. G.; Papargyris, A. D.; Spiliotis, X. D. *J. Mol. Catal.* **1993**, *84*, 267.
(4) Obuchi, A.; Naito, S.; Onishi, T.; Tamaru, K. *Surf. Sci.* **1983**, *130*, 29.
(5) Hirano, H.; Yamada, T.; Tanaka, K. I.; Siera, J.; Cobden, P.; Nieuwenhuys, B. E. *Surf. Sci.* **1992**, *262*, 97.
(6) Siera, J.; Nieuwenhuys, B. E.; Hirano, H.; Yamada, T.; Tanaka, K. I. *Catal. Lett.* **1989**, *3*, 179.
(7) Hecker, W. C.; Bell, A. T. *J. Catal.* **1985**, *92*, 247.
(8) Yao, H. C.; Yao, Y. Y.; Otto, K. *J. Catal.* **1979**, *56*, 21.
(9) Borg, H. J.; Reijerse, J. F. C.-J. M.; Van Santen, R. A.; Niemantsverdriet, J. W. *J. Chem. Phys.* **1994**, *101*, 10052.
(10) Villarrubia, J. S.; Ho, W. *J. Chem. Phys.* **1987**, *87*, 750.
(11) Schmatloch, V.; Kruse, N. *Surf. Sci.* **1992**, *269*/*270*, 488.
(12) Bugyi, L.; Solymosi, F. *Surf. Sci.* **1991**, *258*, 55.
(13) Belton, D. N.; DiMaggio, C. L.; Ng, K. Y. S. *J. Catal.* **1993**, *144*, 273.
(14) Savatsky, B. J.; Bell, A. T. *ACS Symp. Ser.* **1982**, *178*, 105.
(15) Yamada, T.; Tanaka, K. *J. Am. Chem. Soc.* **1991**, *113*, 1173.
(16) Yamada, T.; Hirano, H.; Tanaka, K.; Siera, J.; Nieuwenhuys, B. E. *Surf. Sci.* **1990**, *226*, 1.
(17) Zemlyanov, D. Y.; Smirnov, M. Y.; Gorodetskii, V. V.; Block, J. H. *Surf. Sci.* **1995**, *329*, 61.
(18) Prasad, J.; Gland, J. L. *J. Am. Chem. Soc.* **1991**, *113*, 1577.
(19) Gland, J. L.; Fisher, G. B.; Mitchell, G. E. *Chem. Phys. Lett.* **1985**, *119*, 89.
(20) Bassignana, I. C.; Wagemann, K.; Küppers, J.; Ertl, G. *Surf. Sci.* **1986**, *175*, 22.
(21) Mieher, W. D.; Ho, W. *Surf. Sci.* **1995**, *322*, 151.
(22) Wagner, M. L.; Schmidt, L. D. *J. Phys. Chem.* **1995**, *99*, 805.
(23) Cholach, A. R.; Sobyanin, V. A. *React. Kinet. Catal. Lett.* **1984**, *26*, 381.
(24) Rausher, H.; Kostov, K. L.; Menzel, D. *J. Chem. Phys.* **1993**, *177*, 473.
(25) Mertens, F.; Imbihl, R. *Nature* **1994**, *370*, 124.
(26) Mertens, F.; Imbihl, R. *Surf. Sci.* **1996**, *347*, 355.
(27) Janssen, N. M. H.; Cobden, P. D.; Nieuwenhuys, B. E.; Ikai, M.; Mukai, K.; Tanaka, K. *Catal. Lett.* **1995**, *35*, 155.
(28) Janssen, N. M. H.; Nieuwenhuys, B. E.; Ikai, M.; Tanaka, K.; Cholach, A. R. *Surf. Sci.* **1994**, *319*, L29.
(29) Gierer, M.; Mertens, F.; Over, H.; Ertl, G.; Imbihl, R. *Surf. Sci.* **1995**, *339*, L903.
(30) Cholach, A. R.; Van Tol, M. F. H.; Nieuwenhuys, B. E. *Surf. Sci.* **1994**, *320*, 281.
(31) Hayward, D. O.; Trapnell, B. M. W. *Chemisorption*; Butterworth: London, 1964.
(32) Murray, P. W.; Leibsle, F. M.; Thornton, G.; Bowker, M.; Dhanak, V. R.; Baraldi, A.; Kiskinova, M.; Rosei, R. *Surf. Sci.* **1994**, *304*, 48.
(33) Kiskinova, M.; Lizzit, S.; Comelli, G.; Paolucci, G.; Rosei, R. *Appl. Surf. Sci.* **1993**, *64*, 185.
(34) Lizzit, S.; Comelli, G.; Hofmann, Ph.; Paolucci, G.; Kiskinova, M.; Rosei, R. *Surf. Sci.* **1992**, *276*, 144.
(35) Drechsler, M.; Hoinkes, H.; Kaarmann, H.; Wilsch, H.; Ertl, G.; Weiss, M. *Appl. Surf. Sci.* **1979**, *3*, 217.
(36) Van Hardeveld, R. M.; Van Santen, R. A.; Niemantsverdriet, J. W. *Surf. Sci.*, in press.
(37) Borg, H. J.; Niemantsverdriet, J. W. In *Catalysis: a Specialist Periodical Report*; Royal Society of Chemistry: Cambridge, 1994; Vol. 11, p 1.
(38) Brown, A.; Vickerman, J. C. *Surf. Sci.* **1983**, *124*, 267.
(39) Prasad, J.; Gland, J. L. *Surf. Sci.* **1991**, *258*, 67.
(40) Prasad, J.; Gland, J. L. *Langmuir* **1991**, *7*, 722.
(41) Wagner, M. L.; Schmidt, L. D. *Surf. Sci.* **1991**, *257*, 113.
(42) Yates, J. T., Jr.; Thiel, P. A.; Weinberg, W. H. *Surf. Sci.* **1979**, *84*, 427.
(43) Shustorovich, E.; Bell, A. T. *Surf. Sci. Lett.* **1991**, *259*, L791.